CHEMISTRY OF MATERIALS
Cite This: Chem. Mater. 2018, 30, 3813−3818
Article
pubs.acs.org/cm

Oligomer Hydrate Crystallization Improves Carbon Nanotube Memory

Michael T. Chido,[†] Peter Koronaios,[‡] Karthikeyan Saravanan,[‡] Alexander P. Adams,[†] Steven J. Geib,[†] Qiang Zhu,[§] Hari B. Sunkara,[∥] Sachin S. Velankar,[‡] Robert M. Enick,[‡] John A. Keith,[‡] and Alexander Star*[,†]

[†]Department of Chemistry, University of Pittsburgh, Pittsburgh, Pennsylvania 15260, United States
[‡]Department of Chemical and Petroleum Engineering, University of Pittsburgh, Pittsburgh, Pennsylvania 15261, United States
[§]High Pressure Science and Engineering Center, Department of Physics and Astronomy, University of Nevada Las Vegas, Las Vegas, Nevada 89154-4002, United States
[∥]DuPont Industrial Biosciences, Experimental Station E353/227 I, Wilmington, Delaware 19803, United States

Supporting Information

ABSTRACT: Single-walled carbon nanotube (SWCNT) field-effect transistor (FET) devices have potential for memory storage applications. Devices fabricated with semiconducting SWCNT ink using dielectrophoresis were coated with a renewably sourced poly(oxacyclobutane) oligomer. It was found that this oligomer crystallizes with water to form a semicrystalline oligomer hydrate material. Crystallization also occurs on the SWCNT device surface in ambient conditions, resulting in dramatically increased hysteresis of the SWCNT-FET I-Vg curves. Using alternating current impedance measurements, we found that the oligomer hydrate crystals store charge, acting as a capacitor encapsulating the nanotube network. This capacitive material can serve to electrostatically gate the SWCNT network. The charge storage properties of the oligomer hydrate crystals were applied to store "0" and "1" bits separated by ∼4 orders of magnitude of current. Utilizing powder X-ray diffraction and simulation, we have demonstrated that this semicrystalline material contains aligned, hydrogen-bonded one-dimensional columns of water molecules which allows for charging of the material through electrostatic gating by mobile protons in the crystal structure.

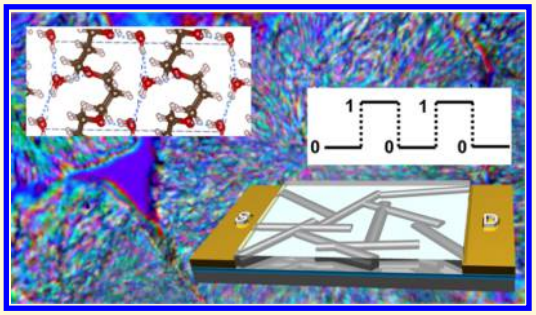

Because of their superior electronic properties,[1,2] nanometer-sized dimensions,[3] and mechanical strength,[4] single-walled carbon nanotubes (SWCNTs) have been applied in a wide array of applications spanning many fields of chemistry and engineering. In particular, SWCNTs have shown to be a promising material when used in field-effect transistor (FET) devices for chemical[5] and biological[6] sensing, high-performance electronics,[7,8] and memory storage materials.[9−12] SWCNTs are synthesized as a mixture of semiconducting and metallic nanotubes, but high-performance FET devices require the removal of metallic nanotube species.[13,14] Removal of metallic species allows for low-power operation by decreasing the current flowing through devices in the off state to nearly zero.[15] Decreasing off current also allows for dramatic improvement of the on/off current, defined as the maximum current in the on state divided by the off current. A high on/off ratio allows for more separated on and off states which is a necessary requirement for high-performance transistor-based memory. High-purity semiconducting SWCNT (s-SWCNT) inks have become increasingly available commercially and this availability allows for cutting edge research with the development of highly pure s-SWCNT-FET devices.

It is known that the transport properties of SWCNT-FETs are heavily influenced by the environment when operated in ambient conditions.[16,17] When SWCNT-FETs are measured in ambient conditions, they act as p-type semiconductors,[18] thought to be a result of their interaction with ambient oxygen and water leading to direct doping effects from oxygen molecules and the creation of low-lying trap states due to the water redox couple.[17] For traditional back-gated SWCNT-FETs, the presence of water on the gate oxide surface and SWCNT network surface is undesirable as it introduces large hysteresis effects during operation.[16] For memory storage applications, hysteresis is a necessary property of a material as it allows for the storage of information. In transistors with hysteresis, the threshold voltage is dependent on the measurement conditions such as the direction in which gate voltage is swept. This difference in threshold voltage is also known as the memory window, and in memory applications, a large memory window is desirable. Memory can be generally classified as nonvolatile memory (NVM) or volatile memory (VM). NVM

Received: March 5, 2018
Revised: May 22, 2018
Published: May 22, 2018

DOI: 10.1021/acs.chemmater.8b00964
Chem. Mater. 2018, 30, 3813−3818

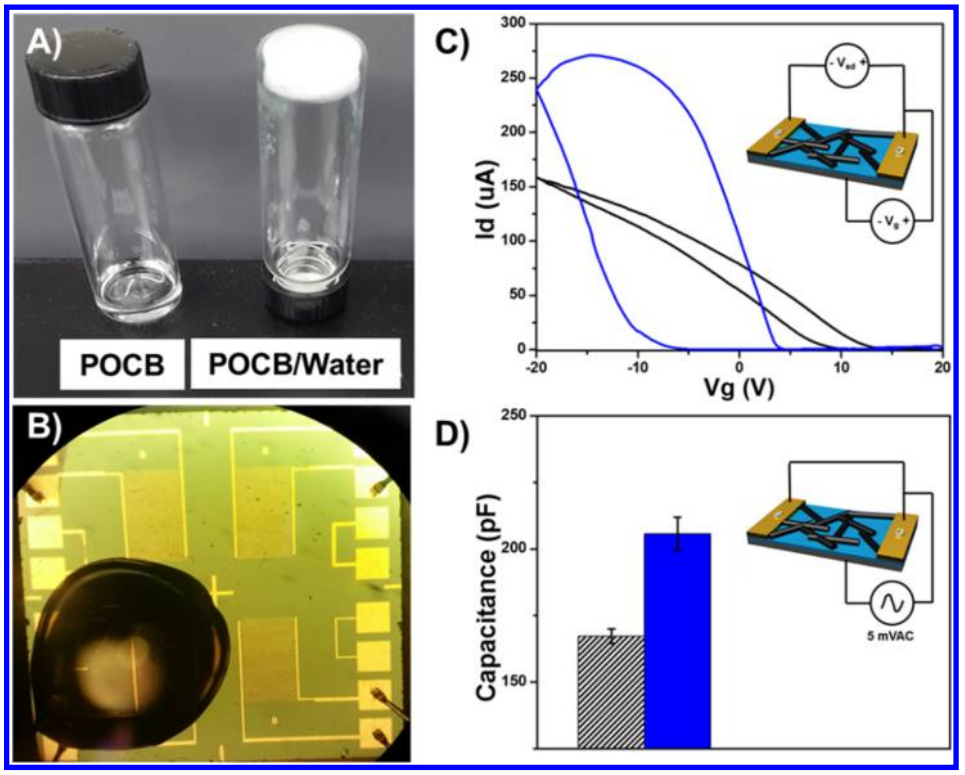

Figure 1. (A) POCB/water mixture completely crystallized. (B) Optical microscope image of a device coated with POCB. (C) s-SWCNT device measured in ambient (black) and after coating with POCB (blue). A large improvement in device performance was observed. (D) Capacitance of the nanotube network (black) and after coating with POCB (blue) showing an increase in capacitance of 38 pF.

materials store information and retain this stored data even after power cycling, whereas VM stores information but loses this information when not powered. SWCNT-FET-based memory devices have been demonstrated in the literature as promising NVM and VM materials.[9−12,19−23] Generally, these devices work by trapping charge, either in the gate oxide[19] or in a passivation coating applied to the SWCNT network.[11,22] NVM devices have slow charge recombination while VM devices quickly recombine charge. In this work, we take advantage of the capacitance of an oligomer/water cocrystalline coating to induce hysteresis in s-SWCNT-FET devices. The capacitance electrostatically gates the s-SWCNTs and produces a large difference in current between the two states in the hysteresis loop at zero gate voltage. The states are separated by nearly 4 orders of magnitude in current, making this simple material suitable for memory storage.

We utilized poly(oxacyclobutane) (POCB), also known as poly(trimethylene oxide), poly(trimethylene ether) glycol, poly(1,3-propanediol), poly(oxetane), or poly(propylene glycol) with a linear monomeric repeat unit, with a number average molecular weight of 650, which spontaneously forms oligomer hydrate crystals with water at room temperature. The crystals melt at 38 °C, far above the melting temperature of either the oligomer (14 °C) or water. Unlike prior reports of POCB hydrates using high molecular weights that are solid at room temperature,[24] to our knowledge, this is one of the only examples of two substances that are liquid at room temperature and spontaneously freeze upon mixing at room temperature.

At room temperature, POCB completely cocrystallizes with water at a water:monomer ratio of 1:1 (1:3 weight ratio) to form a white solid (Figure 1A). The FET devices used in this work were fabricated by photolithography (Figure S1, Supporting Information), and s-SWCNT ink[25] (Isosol-S100, Raymor Industries Inc.) was deposited between source and drain electrodes using dielectrophoresis (details in Supporting Information). The s-SWCNT ink was used as received, and the purity of semiconducting content was evaluated by Raman spectroscopy (Figure S2) and agreed well with previously reported results.[25−27] The devices were operated in a bottom contact, bottom gate configuration. When POCB was deposited on an s-SWCNT-FET device (Figure 1B), excess oligomer spontaneously crystallized with the trace water present on the surface of the silicon oxide and the carbon nanotube network. This process caused a dramatic change in FET transfer characteristics of the device (Figure 1C). An increase in hysteresis was observed after coating and incubation for 1 h. This incubation allows for stabilization of the device as the FET curve immediately after coating changes during the first hour, likely due to equilibration with ambient humidity (Figure S2). This magnitude of hysteresis in the POCB-coated FET devices can be described by a parameter called the memory window which was observed to be 15 V (Figure 1C). Notably, the POCB-coated device displayed ambipolar transport characteristics as well which is better illustrated when the *y*-axis is plotted in a logarithmic scale (Figure S3). This indicates that the trap effect of water presence on the nanotube surface is removed. It has been shown that the p-type conduction in SWCNT-FETs operated in ambient is mostly due to the oxygen−water redox couple whose energy level lies near the conduction band of the CNTs.[17] This available trap state causes poor gate control over electron conduction in SWCNT-FETs.[17] We hypothesized that the increase in hysteresis of POCB-coated devices was caused by capacitive charging effects of POCB crystals electrostatically gating the s-SWCNTs. This capacitive charging was investigated by applying alternating current (ac) impedance measurements to quantify the change in capacitance after

DOI: 10.1021/acs.chemmater.8b00964
Chem. Mater. 2018, 30, 3813−3818

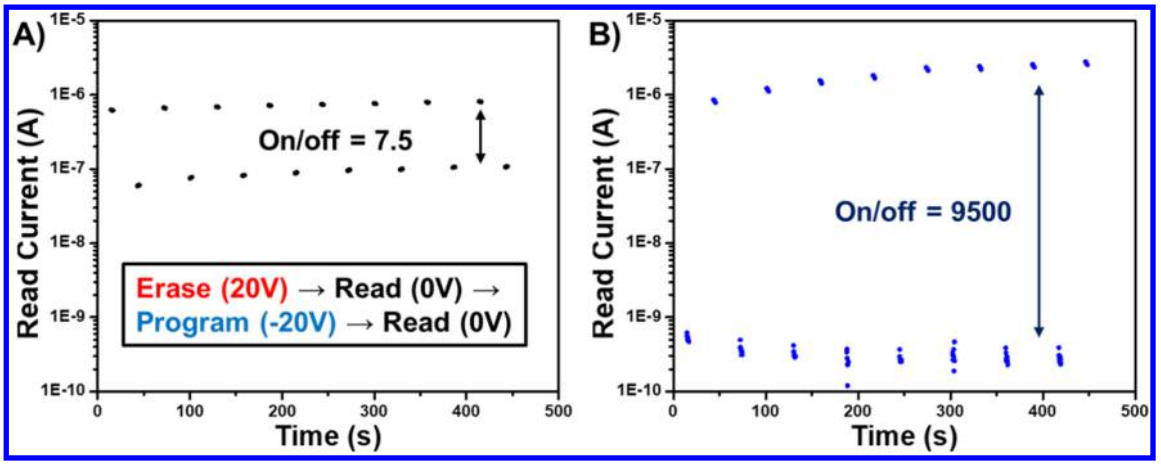

Figure 2. Application of POCB-coated s-SWCNT-FET devices for memory storage. (A) s-SWCNT-FET device showing bit separation of ∼10 with voltages applied for E/R/P/R cycles (inset). (B) POCB-coated s-SWCNT-FET device showing bit retention and separation of $\sim 10^4$.

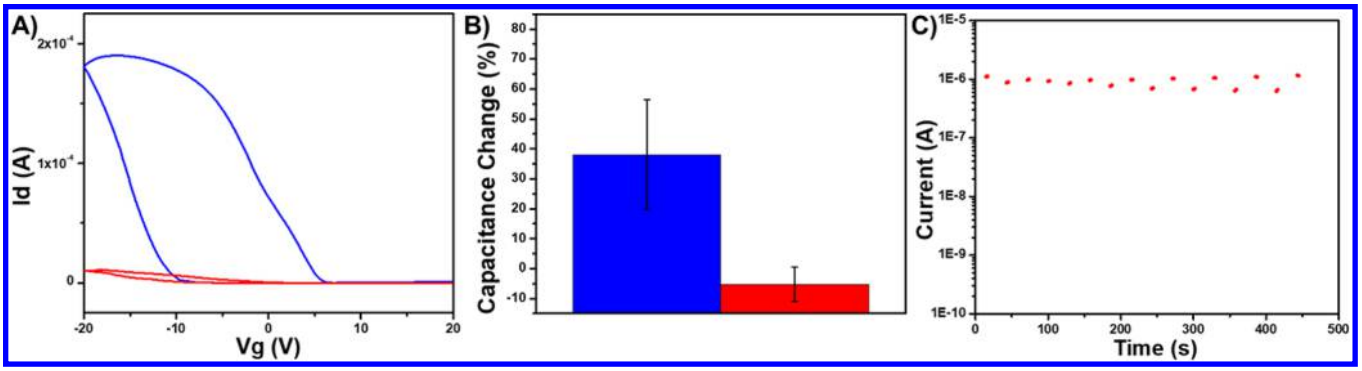

Figure 3. Characterization of POCB-coated devices before (blue) and after (red) removal of water by heating. (A) FET curves indicate that the large hysteresis observed in POCB-coated devices is dependent on POCB-hydrate crystal formation. (B) Change of capacitance compared with an s-SWCNT-FET device before POCB coating showed an increase in capacitance after coating with POCB and the loss of capacitance after heating. (C) Memory test of a heated POCB-coated device showing bit separation failure.

POCB coating. By applying a 5 mV ac wave through the gate oxide and detecting the −90° out-of-phase impedance with a lock-in amplifier, we quantified the total capacitance of the s-SWCNT-FET device before and after POCB coating and found an increase in overall capacitance (Figure 1D). The capacitance of the s-SWCNT-FET device of 167 pF represents the capacitive contribution of the 300 nm SiO_2 insulating gate oxide and the capacitance of the surfactant-coated s-SWCNT network. After POCB coating on the same device, the capacitance increased by 38 pF. This contribution is from the POCB/water crystal material on the oxide surface that acts as a parallel capacitive pathway to the s-SWCNTs, represented as a higher overall capacitance value.

The current separation at a zero-gate voltage in the FET hysteresis loop was on the order of $\sim 10^4$ amps (Figure S3). Because of this and the large memory window of 15 V, we applied this material for memory storage. We utilized the gate voltage parameters used in FET to design a transistor-based capacitive memory cell. Ideally, memory cells are read at zero gate potential to avoid charging effects. These charging effects at non-zero read voltages can lead to significant drift and unwanted collapse of the stored states. On the basis of our FET characterization of POCB-coated s-SWCNT-FET devices, we utilized a 5 s + 20 V gate pulse to erase, which puts the device in the low current state at zero gate voltage. A bit is "programmed" by a 5 s−20 V gate pulse. All bits were read 12 s after the program and erase pulses while applying zero gate voltage (Figure 2A, inset).

First, an s-SWCNT device was tested in ambient conditions without the POCB coating (Figure 2A). Because of the hysteresis present in the s-SWCNT-FET devices measured in ambient conditions (Figures S4 a nd S5), two current states were observed in the memory tests. The separation of the bits, described by an on/off current ratio of "1" divided by "0," was less than 10 which is far below the ideal bit separation of high-performance memory devices (at least 10^3 to 10^4). After a POCB coating was applied to the same device, a dramatic improvement in bit separation was observed (Figure 2B). Interestingly, the 1 and 0 states of the bare s-SWCNT-FET device were reversed when compared to those of the POCB-coated devices.

Bit storage was stable over the eight cycles tested and demonstrated low and stable off currents of ∼300 pA (at the limit of detection of our probing station setup). Longer cycle tests were performed on the POCB devices and they were found to endure at least 100 cycles even after 3 months of storage (Figure S6). This long-term stability suggests the potential application of this material in nonvolatile memory applications.

The retention time of memory storage devices is important because it determines the amount of time that a bit of memory can be stored before being refreshed. The bit retention for the 20 V erase (+20 V) and program (−20 V) of both 1 and 0

DOI: 10.1021/acs.chemmater.8b00964
Chem. Mater. 2018, 30, 3813−3818

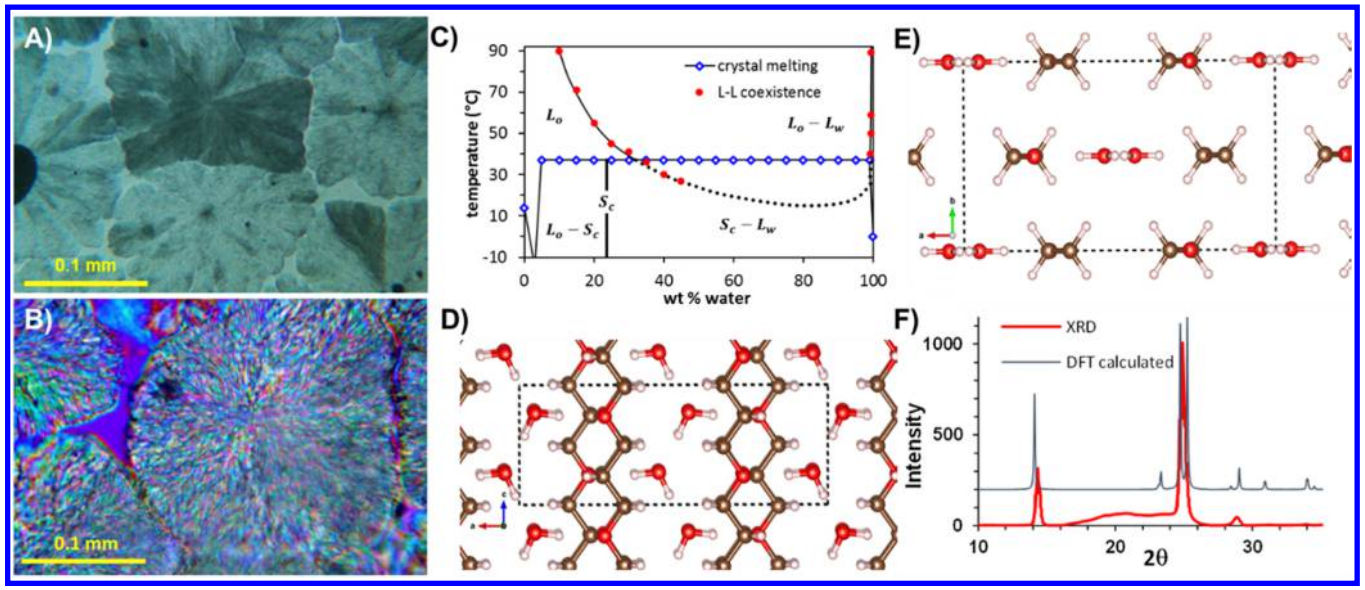

Figure 4. Characterization of POCB/water crystals. (A) Optical microscope image of POCB/water spherulite crystals, indicating semicrystalline morphology. (B) Crystals under a polarization microscope showing birefringence, a common property of semicrystalline polymer materials. (C) Phase diagram of POCB/water binary mixtures at 1 atm based on L−L (liquid−liquid) phase boundary data and solid melting point data. S_c, L_o, and L_w refer to the solid cocrystal phase, oligomer-rich liquid phase, and water-rich liquid phases, respectively. (D) Calculated oligomer hydrate structure showing aligned one-dimensional (1-D) columns of water molecules oriented vertically. Atom color coding is as follows: carbon (brown), oxygen (red), and hydrogen (white). (E) A top down perspective showing 1-D aligned columns of water molecules. (F) Powder X-ray diffraction (XRD) data from crystal compared to the spectrum obtained using density functional theory (DFT).

states was tested to observe the transient behavior of the two states. After 1 h, the current states were still separated by more than an order of magnitude (Figure S7). We also tested the POCB-coated device with 5 V erase (+5 V) and program (−5 V) steps and found that the on/off ratio decreased by an order of magnitude, though the bit separation decreased to 10 after 20 min (Figure S8).

We found that the existence of oligomer crystals is vital for high hysteresis to be observed in the s-SWCNT devices. Removing water by heating at temperatures in excess of 100 °C destroys the POCB-hydrate crystals as water is critical for the crystal formation. A POCB-coated s-SWCNT device FET transfer curve was taken, the device was heated at 120 °C for 1 h in an oven and allowed to cool to room temperature, and another FET transfer curve was taken. We observed that the hysteresis of the device after heating was dramatically decreased and the device properties deteriorated (Figure 3a).

This effect was also observed when looking at the capacitance of the devices using impedance measurements. In a comparison to the s-SWCNT-FET devices before coating, the POCB coating caused an increase in the capacitance of the material. After heating, this increase in capacitance dropped back to pre-POCB coating levels (Figure 3b). We also observed that the memory effect in heated devices was lost, indicating that the presence of the hydrate crystals is critical (Figure 3c). The large increase in bit separation and hysteresis with the POCB-coated devices is due to the capacitive charging of the POCB hydrate crystals, and Figure 3 shows that in the absence of these POCB hydrate crystals, the bit separation is poor and the device is not suitable for memory applications. We also measured memory cycles of a structurally similar oligomer of comparable molecular weight, poly(tetrahydrofuran) 650 (p(THF)), which does not form oligomer hydrates (Figure S9). Compared to POCB devices, the p(THF) device showed 2 orders of magnitude decrease of current separation, indicating the importance of the water cocrystals for SWCNT memory. After a program or erase voltage pulse is applied, the POCB charges up, causing a local electrostatic gating environment near the nanotube surface. This charge cannot be easily compensated by the SWCNT because of the presence of a polymer layer on the surface of the s-SWCNTs, which is likely acting as a tunneling barrier.[22] At larger applied voltages, this separation between both on and off states becomes larger as more charge is built up at larger applied voltages.

We sought to investigate the properties of the POCB−water solid material to further understand the capacitance observed in the material. POCB, an oligomer synthesized by DuPont from renewable materials,[28] is a clear liquid with a viscosity of 325 mPa at 25 °C. DuPont observed the spontaneous formation of a "gel" upon combination of water with POCB of molecular weight 510−820, but the "gel" was not characterized beyond how quickly it returned to liquid form when heated to 40 °C. POCB has several close analogues: poly(ethylene glycol) $[CH_2-CH_2-O-]_x$, poly(tetramethylene glycol), or p(THF) $[CH_2-CH_2-CH_2-CH_2-O-]_x$, and poly(1,2-propane diol) $[CH_2-CH_2(CH_3)-O-]_x$, but none of these cocrystallize with water. This hydrate crystal structure was first observed and characterized by Tadokoro and co-workers (under the name poly(oxacyclobutane)), where molten samples of high molecular weights of POCB were quenched in ice water.[24]

POCB 650 and water form solids over a wide range of mixture compositions. With the exception of the 25 wt % water + 75 wt % POCB mixture, which appeared to be almost dry, the formed solid appeared to be either a wet pastelike solid or solid particles suspended in clear liquid. The freezing process was observed using optical microscopy. A small amount of the dry mixture described previously was placed on a microscope slide and sealed with a coverslip. The solid that formed within 2−5 min on the slide was composed of spherulites (Figure 4a). This morphology is typical for semicrystalline polymers and

DOI: 10.1021/acs.chemmater.8b00964
Chem. Mater. 2018, 30, 3813−3818

unambiguously establishes that the solid is crystalline. In semicrystalline polymers, each spherulite normally consists of 5−30 nm thick lamellar crystals radiating outward from the center of the spherulite with amorphous regions between the lamellae[29] and the same microstructure is expected here. The spherulites appeared birefringent under a polarization microscope, which is common among polymeric crystals (Figure 4b).

The phase behavior of the POCB/water mixtures at ambient pressure was investigated utilizing cloud point data, melting point data, and an NMR-based estimate of water content in the solid crystal (Figures S10−S12). A phase diagram for the binary mixture was constructed on the basis of these experiments (Figure 4c). The experimental details can be found in the Supporting Information.

Since the POCB/water solid samples are not single crystals, but polycrystalline, powder X-ray diffraction (XRD) can be expected to observe all orientations as would be observed from computationally obtained XRD spectra. Experimental powder XRD on the polycrystalline samples matched our calculated spectra from quantum chemistry modeling using the POCB hydrate structure reported by Tadokoro and co-workers.[24] Alternative POCB hydrate structures were investigated using the USPEX code[30] (Figure 4f), but these did not match the experimental XRD spectra. The calculated energy values were higher than Tadokoro's structure (details in Supporting Information). The hydrate structure exhibits 1-D chains of water molecules running through the cocrystal (Figure 4d,e). We propose that these 1-D aligned channels of water molecules, which are in a hydrogen-bonded network,[24] allow for proton conductivity in the POCB hydrate crystals. This type of oligomer crystalline structure has been studied for proton conductivity for other polymer hydrates previously.[31] In this study, the authors found that with the ionic conductivity in crystalline hydrates of linear poly(ethylenimine) the main carriers of charge were likely protons. They found that ionic conduction in this hydrate material should primarily occur within the crystalline phases of the amorphous material and that hydrogen bonding played a critical role in the ionic conduction.[31] We have shown that POCB hydrate crystals can be capacitively charged with applied voltage bias, which is likely the result of biased proton conductivity in the material. Having the charged species near the SWCNT network electrostatically gates the nanotubes. The hysteresis observed in the FET of the POCB-coated devices (Figure 1C) is due to the charging and discharging process of the POCB/water cocrystals lagging behind the applied gate voltage. This effect was observed for clockwise and counterclockwise I-Vg sweeps to give very similar transfer curves as is expected for this phenomenon (Figure S4). The lagging effect is also seen in the FET curves of POCB-coated devices in Figure 1C and 3A as the highest output current occurs after we sweep past the largest negative gate voltage.

In conclusion, we found that coating s-SWCNT-FET devices with POCB causes a dramatic increase in hysteresis. This hysteresis can be utilized for memory storage devices with a bit separation of ~10^4. These devices perform well when compared to other carbon nanotube-based field-effect transistor memory devices (Table S1). POCB displays very interesting phase behavior[32] and crystallizes with water at room temperature to form structures with hydrogen-bonded 1-D chains of water molecules propagating through the structure. We believe that this structure allows for trapping and shuttling of charge under applied gate bias by proton migration in the oligomer hydrate crystals which is the cause of the large observed hysteresis in s-SWCNT-FET measurements. This material represents a simple and effective way to store information in nanoelectronic transistor devices. Although we propose this material for nonvolatile memory applications, further improvement would be required for implementation for reliable memory storage. Specifically, a decrease in the applied voltage amplitude for writing/erasing as well as longer retention times are desirable properties for nonvolatile memory. We have demonstrated bit retention to at least 1 h, and ideally this would be many years in order to compete with current silicon-based memory technologies. There is potential for further optimization of these devices by using high-k dielectric gate oxides (i.e., HfO_2) to improve applied voltage efficiency, allowing for lower voltage devices. Improving the gate oxide would likely also improve the voltage pulse times required for writing and erasing. Device design and size also likely have an effect on how efficiently the POCB−water crystalline material can electrostatically gate the s-SWCNT FET material and we believe that improvements could be made through careful optimization of these parameters.

■ ASSOCIATED CONTENT

Supporting Information

The Supporting Information is available free of charge on the ACS Publications website at DOI: 10.1021/acs.chemmater.8b00964.

Photolithography of devices, field-effect transistor measurements, ac impedance measurements, memory testing, phase behavior studies, solid-state NMR, X-ray crystallography, and DFT calculations (PDF)

■ AUTHOR INFORMATION

Corresponding Author

*E-mail: astar@pitt.edu.

ORCID

Steven J. Geib: 0000-0002-9160-7857
Qiang Zhu: 0000-0002-9892-0344
Hari B. Sunkara: 0000-0001-5870-894X
Sachin S. Velankar: 0000-0001-7541-1355
John A. Keith: 0000-0002-6583-6322
Alexander Star: 0000-0001-7863-5987

Notes

The authors declare no competing financial interest.

■ ACKNOWLEDGMENTS

We thank Dr. Jianfu Ding and Dr. Patrick Malenfant at the National Research Council of Canada for providing high-purity seminconducting single-walled carbon nanotubes. Sachin Velankar is thankful for funding support from the Mascaro Center for Sustainable Innovation at the University of Pittsburgh.

■ REFERENCES

(1) Javey, A.; Guo, J.; Wang, Q.; Lundstrom, M.; Dai, H. Ballistic Carbon Nanotube Field-Effect Transistors. *Nature* **2003**, *424*, 654−657.

(2) White, C. T.; Todorov, T. N. Carbon Nanotubes as Long Ballistic Conductors. *Nature* **1998**, *393*, 240−242.

(3) Iijima, S. Helical Microtubules of Graphitic Carbon. *Nature* **1991**, *354*, 56−58.

DOI: 10.1021/acs.chemmater.8b00964
Chem. Mater. 2018, 30, 3813−3818

(4) Treacy, M. M. J.; Ebbesen, T. W.; Gibson, J. M. Exceptionally High Young's Modulus Observed for Individual Carbon Nanotubes. *Nature* **1996**, *381*, 678−680.
(5) Kauffman, D. R.; Star, A. Carbon Nanotube Gas and Vapor Sensors. *Angew. Chem., Int. Ed.* **2008**, *47*, 6550−6570.
(6) Münzer, A. M.; Michael, Z. P.; Star, A. Carbon Nanotubes for the Label-Free Detection of Biomarkers. *ACS Nano* **2013**, *7*, 7448−7453.
(7) Sun, D.-M.; Timmermans, M. Y.; Tian, Y.; Nasibulin, A. G.; Kauppinen, E. I.; Kishimoto, S.; Mizutani, T.; Ohno, Y. Flexible High-Performance Carbon Nanotube Integrated Circuits. *Nat. Nanotechnol.* **2011**, *6*, 156−161.
(8) Cao, Q.; Kim, H.-S.; Pimparkar, N.; Kulkarni, J. P.; Wang, C.; Shim, M.; Roy, K.; Alam, M. A.; Rogers, J. A. Medium-Scale Carbon Nanotube Thin-Film Integrated Circuits on Flexible Plastic Substrates. *Nature* **2008**, *454*, 495−500.
(9) Fuhrer, M. S.; Kim, B. M.; Dürkop, T.; Brintlinger, T. High-Mobility Nanotube Transistor Memory. *Nano Lett.* **2002**, *2*, 755−759.
(10) Rinkiö, M.; Johansson, A.; Paraoanu, G. S.; Törmä, P. High-Speed Memory from Carbon Nanotube Field-Effect Transistors with High-κ Gate Dielectric. *Nano Lett.* **2009**, *9*, 643−647.
(11) Star, A.; Lu, Y.; Bradley, K.; Grüner, G. Nanotube Optoelectronic Memory Devices. *Nano Lett.* **2004**, *4*, 1587−1591.
(12) Rueckes, T.; Kim, K.; Joselevich, E.; Tseng, G. Y.; Cheung, C.-L.; Lieber, C. M. Carbon Nanotube-Based Nonvolatile Random Access Memory for Molecular Computing. *Science* **2000**, *289*, 94−97.
(13) Collins, P. G.; Arnold, M. S.; Avouris, P. Engineering Carbon Nanotubes and Nanotube Circuits Using Electrical Breakdown. *Science* **2001**, *292*, 706−709.
(14) Zhang, G.; Qi, P.; Wang, X.; Lu, Y.; Li, X.; Tu, R.; Bangsaruntip, S.; Mann, D.; Zhang, L.; Dai, H. Selective Etching of Metallic Carbon Nanotubes by Gas-Phase Reaction. *Science* **2006**, *314*, 974−977.
(15) Javey, A.; Guo, J.; Farmer, D. B.; Wang, Q.; Wang, D.; Gordon, R. G.; Lundstrom, M.; Dai, H. Carbon Nanotube Field-Effect Transistors with Integrated Ohmic Contacts and High-κ Gate Dielectrics. *Nano Lett.* **2004**, *4*, 447−450.
(16) Kim, W.; Javey, A.; Vermesh, O.; Wang, Q.; Li, Y.; Dai, H. Hysteresis Caused by Water Molecules in Carbon Nanotube Field-Effect Transistors. *Nano Lett.* **2003**, *3*, 193−198.
(17) Qian, Q.; Li, G.; Jin, Y.; Liu, J.; Zou, Y.; Jiang, K.; Fan, S.; Li, Q. Trap-State-Dominated Suppression of Electron Conduction in Carbon Nanotube Thin-Film Transistors. *ACS Nano* **2014**, *8*, 9597−9605.
(18) Derycke, V.; Martel, R.; Appenzeller, J.; Avouris, P. Controlling Doping and Carrier Injection in Carbon Nanotube Transistors. *Appl. Phys. Lett.* **2002**, *80*, 2773−2775.
(19) Radosavljević, M.; Freitag, M.; Thadani, K. V.; Johnson, A. T. Nonvolatile Molecular Memory Elements Based on Ambipolar Nanotube Field Effect Transistors. *Nano Lett.* **2002**, *2*, 761−764.
(20) Di Bartolomeo, A.; Rinzan, M.; Boyd, A. K.; Yang, Y.; Guadagno, L.; Giubileo, F.; Barbara, P. Electrical Properties and Memory Effects of Field-Effect Transistors from Networks of Single- and Double-Walled Carbon Nanotubes. *Nanotechnology* **2010**, *21*, 115204.
(21) Cho, B.; Kim, K.; Chen, C.-L.; Shen, A. M.; Truong, Q.; Chen, Y. Nonvolatile Analog Memory Transistor Based on Carbon Nanotubes and C60 Molecules. *Small* **2013**, *9*, 2283−2287.
(22) Hwang, I.; Wang, W.; Hwang, S. K.; Cho, S. H.; Kim, K. L.; Jeong, B.; Huh, J.; Park, C. Multilevel Non-Volatile Data Storage Utilizing Common Current Hysteresis of Networked Single Walled Carbon Nanotubes. *Nanoscale* **2016**, *8*, 10273−10281.
(23) Di Bartolomeo, A.; Yang, Y.; Rinzan, M. B. M.; Boyd, A. K.; Barbara, P. Record Endurance for Single-Walled Carbon Nanotube−Based Memory Cell. *Nanoscale Res. Lett.* **2010**, *5*, 1852−1855.
(24) Kakida, H.; Makino, D.; Chatani, Y.; Kobayashi, M.; Tadokoro, H. Strutural Studies of Polyethers [-(CH2)mO-]n. VIII. Polyoxacyclobutane Hydrate (Modification I). *Macromolecules* **1970**, *3*, 569−578.
(25) Ding, J.; Li, Z.; Lefebvre, J.; Cheng, F.; Dunford, J. L.; Malenfant, P. R. L.; Humes, J.; Kroeger, J. A Hybrid Enrichment Process Combining Conjugated Polymer Extraction and Silica Gel Adsorption for High Purity Semiconducting Single-Walled Carbon Nanotubes (SWCNT). *Nanoscale* **2015**, *7*, 15741−15747.
(26) Ding, J.; Li, Z.; Lefebvre, J.; Cheng, F.; Dubey, G.; Zou, S.; Finnie, P.; Hrdina, A.; Scoles, L.; Lopinski, G. P.; Kingston, C. T.; Simard, B.; Malenfant, P. R. L. Enrichment of Large-Diameter Semiconducting SWCNTs by Polyfluorene Extraction for High Network Density Thin Film Transistors. *Nanoscale* **2014**, *6*, 2328−2339.
(27) Li, Z.; Ding, J.; Finnie, P.; Lefebvre, J.; Cheng, F.; Kingston, C. T.; Malenfant, P. R. L. Raman Microscopy Mapping for the Purity Assessment of Chirality Enriched Carbon Nanotube Networks in Thin-Film Transistors. *Nano Res.* **2015**, *8*, 2179−2187.
(28) Harmer, M. A.; Confer, D. C.; Hoffman, C. K.; Jackson, S. C.; Liauw, A. Y.; Minter, A. R.; Murphy, E. R.; Spence, R. E.; Sunkara, H. B. Renewably Sourced Polytrimethylene Ether Glycol by Superacid Catalyzed Condensation of 1,3-Propanediol. *Green Chem.* **2010**, *12*, 1410−1416.
(29) Hiemenz, P. C.; Lodge, T. P. Crystalline Polymers. In *Polymer Chemistry*; CRC Press: Boca Raton, FL, 2007; Chapter 13, p 511.
(30) Zhu, Q.; Sharma, V.; Oganov, A. R.; Ramprasad, R. Predicting Polymeric Crystal Structures by Evolutionary Algorithms. *J. Chem. Phys.* **2014**, *141*, 154102.
(31) Watanabe, M.; Ikezawa, R.; Sanui, K.; Ogata, N. Protonic Conduction in Poly(ethylenimine) Hydrates. *Macromolecules* **1987**, *20*, 968−973.
(32) Banerjee, J.; Koronaios, P.; Morganstein, B.; Geib, S. J.; Enick, R. M.; Keith, J. A.; Beckman, E. J.; Velankar, S. S. Liquids That Freeze When Mixed: Cocrystallization and Liquid−Liquid Equilibrium in Polyoxacyclobutane−Water Mixtures. *Macromol.* **2018**, *51*, 3176−3183.

DOI: 10.1021/acs.chemmater.8b00964
Chem. Mater. 2018, 30, 3813−3818